Intraseasonal Kelvin Waves in Makassar Strait

Kandaga Pujiana[1] and Arnold L. Gordon

Lamont-Doherty Earth Observatory, Palisades, New York

Janet Sprintall

Scripps Institution of Oceanography, La Jolla, California

[1] *Corresponding author address*: Kandaga Pujiana, Lamont-Doherty Earth Observatory, 61 Route 9W, Palisades, NY 10964.
E-mail: kandaga@ldeo.columbia.edu

Abstract

Time series observations during 2004-2006 reveal the presence of 60-90 days intraseasonal events that impact the transport and mixing environment within Makassar Strait. The observed velocity and temperature fluctuations within the pycnocline reveal the presence of Kelvin waves including vertical energy propagation, energy equipartition, and non-dispersive relationship. Two current meters at 750 m and 1500 m provide further evidence that the vertical structure of the downwelling Kelvin wave resembles that of the second baroclinic wave mode. The Kelvin waves derive their energy from the equatorial Indian Ocean winds, including those associated with the Madden-Julian Oscillations, and propagate from Lombok Strait to Makassar Strait along the 100-m isobath. The northward propagating Kelvin Waves within the pycnocline reduce the southward Makassar Strait throughflow by up to 2 Sv and induce a vertical mixing rate of 1-5x10^{-5} m^2s^{-1}.

1. Introduction

The Makassar Strait (Fig. 1) throughflow is a prominent component of the Indonesian Throughflow (ITF; Gordon et al., 1996, 2003, and 2005). Makassar strait is not only the main inflow conduit for the ITF (Gordon et al., 2008 and 2010) but also part of a waveguide extending along the equatorial Indian Ocean to the southwestern coasts of Indonesia then to Makassar Strait, via Lombok Strait (Fig. 1; Wijffels and Meyers, 2004). Previous modeling studies have discussed the role of the waveguide in connecting wind energy in the equatorial Indian Ocean to the Makassar Strait throughflow variability with timescales varying from semiannual to intraseasonal (Qiu et al., 1999; Sprintall et al., 2000; Schiller et al., 2010; Shinoda et al., 2012). The studies of Sprintall et al. (2000) and Shinoda et al. (2012) argued that semiannual variations (180 day) in the equatorial Indian Ocean zonal winds induced a response in the South Java Current (SJC) through coastally trapped Kelvin waves (CTKWs). The semiannual CTKWs propagate farther east along the southern coasts of Indonesian archipelago into the Savu Sea, but part of the wave energy is transmitted through the narrow Lombok Strait, which then move equatorward to force northward Makassar Strait throughflow. At intraseasonal timescales (20-90 days), Qiu et al. (1999) and Schiller et al. (2010) modeled the intraseasonal variation in the Indo-Pacific region and proposed that the equatorial Indian Ocean wind-forced CTKWs also accounted for intraseasonal variability in the ITF passages. These modeling studies emphasized the ITF reversal event as an indicator of the CTKW passage in Makassar Strait but did not elaborate on the mechanism of the CTKW transmission from Lombok Strait to Makassar Strait.

Observations during December 1996 - June 1998 from two current meters (Fig. 1) at depths of 250 m and 350 m in Makassar Strait revealed that the subinertial flow was marked with northward (positive) along-strait flow in May 1997, during which strong intraseasonal northward flow completely reversed the southward lower-frequency background flow (Fig. 2). In addition to the May-June 1997 event, intraseasonal variability's most pronounced impact to attenuate the southward Makassar Strait throughflow was observed in December 1996 and 1997, September, October 1997, and January, February, March, April 1998 (Fig. 2).

Analyzing along-strait flow data within the pycnocline in Makassar Strait and Lombok Strait observed during the INSTANT 2004-2006 program (Gordon et al., 2008; 2010, Sprintall et al., 2009) and zonal current data from a mooring in the eastern equatorial Indian Ocean, Pujiana et al. (2009) found a coherent signal at intraseasonal timescales propagating from the equatorial Indian Ocean to Makassar Strait through Lombok Strait with the speed consistent with that of a baroclinic wave. Drushka et al. (2010), focusing their analyses on the vertical structure of along-strait flow at the outflow passages of the ITF, indicated that the intraseasonal along-strait motions at Lombok Strait had a vertical structure of a remotely wind-forced Kelvin wave.

In this study we utilize the 2004-2006 Makassar Strait dataset to investigate intraseasonal features consistent with the theoretical Kelvin wave characteristics, specifically those of the downwelling Kelvin waves forcing the northward along-strait flow events, and evaluate the likely pathway channeling the intraseasonal energy from Lombok to Makassar Straits. Moreover the Kelvin wave's impact on the ITF variability and mixing environment in Makassar Strait are addressed.

The paper is organized as follows. The data description is given in Section 2, followed in Section 3 with a discussion of the evidence supporting the intraseasonal Kelvin wave variability. The waveguide pathway from Lombok Strait to Makassar Strait is discussed in Section 4. The Kelvin wave's influence on the Makassar throughflow transport and mixing is evaluated in Section 5. A discussion and summary follow in Section 6.

2. Data

2.1 Makassar Strait Mooring in situ data

We employ the velocity and temperature datasets obtained during the INSTANT 2004-2006 program to identify intraseasonal Kelvin wave events in Makassar Strait. The INSTANT program monitored the ITF variability in Makassar Strait at two moorings: 2°51.9' S, 118° 27.3 E [Mak-West] and 2°51.5' S, 118° 37.7' E [Mak-East], within the 45 km wide Labani Channel (Gordon et al., 2008; Fig. 1). An upward-looking RD Instruments Long Ranger 75 kHz Acoustic Doppler Current Profiler [ADCP] at a depth of 300 m and three current meters at 200, 400, and 750 m on each mooring (the Mak-west mooring had an additional current meter at 1500 m) recorded the velocity data with a sampling period of 0.5-2 hour. Both moorings fully resolve the vertical structure of the horizontal velocity across the pycnocline depths of 50-450 m almost continuously (other than a short gap between recovery and redeployment on 7-10 July 2005) for a ~3-year long period from January 2004 to through November 2006. The horizontal current vectors are subsequently projected to the along (y) and across-strait (x) axis of the Labani Channel, which are oriented along -10° and 80° (relative to north and positive is clockwise) respectively (Fig.1), to yield gridded along (v) and across-strait (u) currents. In addition to the moored velocity datasets in Makassar Strait, we also use the hourly velocity data at pycnocline depth of 50-150 m from INSTANT moorings in Lombok Strait (Fig. 1. For more information on the Lombok mooring configurations, see Sprintall et al., 2004 and 2009).

Temperature stratification from 100 to 400 m within the Makassar Strait pycnocline are resolved by the temperature and pressure sensors attached to Mak-West and Mak-East moorings. Mak-West mooring provided higher resolution with 17 sensors attached, while Mak-East mooring only had 5 sensors. Since the vertical structure of temperature variability is less well resolved at the Mak-East mooring, we will only analyze the temperature profile dataset from Mak-West. The sensors sampled temperature and pressure at 6-minute intervals over the entire 3 years INSTANT deployment period. The temperature datasets are linearly interpolated onto a 25-m depth grid for each two-hour time step to provide the gridded temperature data from 150 to 350 m of water column.

2.2 Shallow-pressure gauge and satellite-derived data

In addition to the moored data in Makassar and Lombok Straits, we also employ the sea level anomaly (SLA) data from two shallow pressure gauges (Pw and Pe) in Lombok Strait (Fig. 1) and from the gridded SLA products (merged and delayed time products) of Archiving, Validation, and Interpretation of Satellite Oceanographic Data (AVISO, Ducet et al, 2000). The shallow pressure gauge data are daily, and more information on the pressure gauge setting can be found in Sprintall et al. (2004). The satellite-derived SLA has a horizontal resolution of 0.25° x 0.25° and temporal resolution of 7 days, and the emphasis of our analysis will be on the SLA variability in Lombok Strait and along the southeastern coasts of Indonesia archipelago (Fig.1). Furthermore we will be focusing on the SLA variability during April-June 2004 (Fig. 3), one of the events when both moorings in Makassar and Lombok Straits display strong northward flow. The northward flow observed in Makassar Strait on May 30th 2004 (Fig. 4b-d) was preceded by mass pilling up ($+\eta$) against the southwestern coasts of Sumatra on 12 May, followed up by southeastward propagation of the $+\eta$ signal so that the southern coasts of Java was marked with $+\eta$ on 19 May (Fig. 3). The occurrence of $+\eta$ signal extended from the southern coasts of Java to the mooring sites in Makassar Strait via Lombok Strait on 26 May although there are some concerns on the SLA data quality within the internal Indonesian seas.

3. Intraseasonal variability in Makassar Strait

3.1 Weakened ITF events at intraseasonal timescales

Focusing on the weakened or reversed southward flow in Makassar Strait, the v component at the base of the pycnocline at 450 m depth (Fig. 4d) demonstrates that southward subinertial flow, v^s (low-passed v time series with cut off periods of 9 days) reversed to northward flow five times over the course of 2004-2006: May 2004 and 2005, September 2005 and 2006, and November 2006. Although no ITF reversal was observed at depths shallower than 250 m, the northward v^s phases in May 2004 and 2005 and in November 2006 were observed as shallow as 350 m. One feature consistently revealed within the along channel pycnocline flow is the strong influence of intraseasonal variability, v' (band-passed v timeseries with cut off periods of 20 and 90 days) on v^s: a northward v^s event always corresponds with a northward v' phase (Fig. 4b-d).

Over the course of 2004-2006, there were 17 northward (+v') events with recurring period of 2-3 months (Fig. 4b-d). The +v' during May 2004 and 2005 was the most energetic of all +v' events, while other less energetic +v' events peaked in February, March, August and December 2004; January, March, July, September, and November 2005; January, April, June, August, September, and November 2006. The +v' episodes demonstrated a strong correlation with the zonal winds in the eastern equatorial Indian Ocean (not shown) and those particularly occurring in March and May 2004; May, and September 2005 were preceded by significant MJO phases (Pujiana et al., 2009, Fig. 4a) with the +v' events in Makassar Strait lagging the MJO by 19-25 days (Fig. 4e). Zhou and Murtugudde (2010) conjectured that the MJO influenced the intraseasonal variability at Lombok Strait. They further suggested that the meridional currents were reversed from southward to northward at Lombok Strait 15 days after the day of a peak MJO index. Thus the lag of 19-25 days revealed by +v' in Makassar Strait, with respect to a strong MJO event, indicates a link between the intraseasonal variability in Makassar Strait and MJO episodes. More discussion on the relationship between the +v' events in Makassar Strait and the MJO significant phases are given in Section 6.

3.2 Subpycnocline intraseasonal variability

The v timeseries at 750 m and 1500 m also display significant intraseasonal variability with a diminished subinertial background flow marked with recurring intraseasonal oscillation with a 60-day period (Fig. 5a,b). The intraseasonal variation explains ~80% of the total variance of the subpycnocline current meters v timeseries. Aside from their energetic intraseasonal signatures, the v' at 750 m and 1500 m in Makassar Strait also displays a unique characteristic that is not expected to be observed at depths where the stratification frequency is quasi-homogeneous: the flows at 750 m and 1500 m are out of phase. A lagged correlation between the v' data at 750 m and that at 1500 m shows a statistically significant correlation with $r^2 = -0.8$, and a coherence analysis further indicates that the 60-day oscillation is the most coherent among the v' data at both depths with a phase shift of 180° (not shown).

The time series from the two subpycnocline current meters (Fig. 5a,b) are used to analyze the vertical profiles of v' from 50-1500 m attributed to the $+v'$ events observed in the pycnocline depths (Fig. 4b-d). With over the 17 $+v'$ episodes during 2004-2006, the v' data consistently exhibit a vertical structure which signifies a baroclinic structure with two zero crossing depths, indicative of a second baroclinic wave mode. Examples of the measured v' vertical structure in May, September and November of 2005 when the $+v'$ was maximum are shown in Fig. 5c.

3.3 Kelvin Wave Signatures

As discussed above, intraseasonal motions account for a significant proportion of the variance of the Makassar Strait variability (Figs. 4 and 5) and are clearly evident in the datasets as $+v'$. In this subsection, we provide evidence linking the $+v'$ attributes to theoretical Kelvin wave characteristics such as a vertically propagating wave, normal mode approximation, energy equipartition, and semi-geostrophic balance.

3.3.1 Vertically propagating waves

Over the 17 occasions when v^s turned northward or was greatly attenuated during 2004-2006, one consistent feature was that the *v'* profile across the pycnocline indicated upward phase propagation as +*v'* at deeper levels led that at shallower levels. The composites of the *v'* data, formed by isolating each +*v'* event and then averaging over the set of events observed during 2004-2006, demonstrated weak flow at depths shallower than 100 m, velocity core in the lower thermocline at 200 m at Mak-East and 350 m at Mak-West (Fig. 6). There is an upward phase tilt (dz/dt) associated with the *v'* of 50 m/day (Fig. 6).

What ocean dynamics might force this upward phase propagation of +*v'* events in Makassar Strait? We suggest that this trait is consistent with the dynamics of vertically propagating Kelvin waves. If a wind-forced Kelvin wave perturbed the surface of a stratified ocean, the energy attributed to the perturbation would not only propagate horizontally away from the perturbation point but also downward making a horizontal slope of $\theta = \omega/N = dz/dx$, where ω is a wave frequency, N is stratification frequency, z is depth, and x is horizontal distance. As our composite plots are in depth and time domains, the slope equation can be equivalently written as $dz/dt = \omega.c/N$, where c is a theoretical phase speed of a baroclinic wave mode and t is time. Thus an observer, stationed at a distance away from where a Kelvin wave is generated, would see the linear wave signature arrives deeper in the water column first.

To test whether the observed phase slope (Fig. 6) inferred from the +*v'* composite is consistent with the slope formula, we use an averaged stratification profile (N) from several CTD casts along the projected ray path (Fig. 1). The phase speed (c) is inferred from the normal mode analysis of N (Fig. 1). Given $\omega = 2\pi/(20\text{-}90)$-day, $c = 1.2\text{-}2.5$ m/s (the phase speed for the first two wave modes), and $N = 0.0068$ s^{-1}. Thus dz/dt varies within 15-115 m/day which agrees fairly well with the phase slope inferred from the *v'* composite (Fig. 6). Thus the pattern of upward phase shift with a slope of 50 m/day observed in the *v'* composite likely expresses a linear Kelvin wave signature.

A vertically propagating Kelvin wave can also be identified from how temperature fluctuations and velocity vectors associated with the wave are related. The pressure perturbation (*p'*) and its corresponding vertical velocity (*w'*) for a vertically propagating Kelvin wave are written as $p'(x,y,z,t) = \left(\frac{2}{\pi}\right)\int \hat{p}\cos(mz)\,dm$ and $w' = -(\frac{N^2}{\rho_o})\partial^2 p'/\partial z\partial t$ respectively, where m is vertical wavenumber and ρ_o is background density. Assuming density (ρ') fluctuations can be represented by temperature (*T'*) fluctuations and vertical displacements of density surfaces are solely driven by the vertical velocity following $\partial p'/\partial t + w'\partial\bar{p}/\partial z = 0$, it is implied that the highs and lows of *T'* and *p'* are separated by π/2. Since *p'* is in phase with the wave induced horizontal velocity vectors (*u'*, *v'*), it is also implied that *T'* and (*u'*, *v'*) attributed to a theoretical Kelvin wave would have the same phase shift. Plots of the *v'* and *T'* timeseries for several depths, which focus on an episode of strong +*v'* in late May 2004, demonstrate that maximum northward along-strait flow occurs prior to maximum temperature oscillations with a lead of approximately ¼ cycle (Fig. 7) implying that *T'* would lead *v'* in a space domain by about π/2. This agrees well with the phase relationship required for an upward propagating Kelvin wave.

3.3.2 Normal Mode Approximation

The velocity vectors associated with a theoretical Kelvin wave in a strait are separable into their across-strait and vertical components, and the vertical component can be written as $\frac{\partial^2 v'}{\partial z^2} + \left(\frac{N^2}{c}\right) v' = 0$, where *v'* denotes along-strait flow, *N* is stratification frequency, *c* is baroclinic wave speed. With proper boundary conditions and arbitrary *N*, Gill (1982) suggests that the amplitude and phase of *v'* were proportional to $N^{1/2}\ e^{\pm i(1/c)\int N dz}$ and $\int Ndz$ respectively. The moored datasets in Makassar Strait reveal that *v'* at 200 m is significantly coherent with that at deeper levels for the period band of 45-90 days (see Fig. 5 of Pujiana et al., 2009) and shows the maximum coherence with the 60-day oscillation (Fig. 8a). Furthermore *v'* at 200 m lags that at 450 m by 40° (Fig. 8b). Because the phase difference is proportional to the summation of the magnitudes of *N* with depth between two depth limits, we may define the phase lag between 200 and 450 m as $\theta_{200} - \theta_{450} \sim (\int_{200}^{450} Ndz / \int_{0}^{2000} Ndz)(\theta_0 - \theta_{2000})$. Assume θ_0 - θ_{2200} is the phase difference for a full cycle over the ocean depth (i.e. 360°), the ratio between (θ_{200} - θ_{450}) and (θ_0 - θ_{2000}) should be equivalent to 0.11, which is reasonably close to the measured value of 0.15 given by ($\int_{200}^{450} Ndz / \int_{0}^{2000} Ndz$) (Fig. 8c). The theoretical Kelvin wave solution is thereby applicable to explain the relationship between the observed vertical structure of *v'* and *N*.

3.3.3 Energy Equipartition

As in the oscillation of a pendulum, a theoretical Kelvin wave also expresses equal partition between its corresponding kinetic and potential energies (Pedlosky, 2003). We use the *v'* and *T'* data to examine whether the energy equipartition in the wave field also characterizes the intraseasonal motions observed in the Makassar Strait pycnocline. To estimate the potential energy (PE), the temperature timeseries over several depths ranging the pycnocline of the Mak-West mooring are converted to vertical displacements (η') using a heat equation of $\eta'(z,t)=T'(z,t)/\partial T'/\partial z$, in which horizontal advection, diffusion, and heat sources are neglected. We also remove the effect of static stability on the thermal field through normalizing η' with the ratio between N and its corresponding vertical average N_o, $\eta'_n(z,t) = \eta'(z,t)(N/N_o)$, where z, t, and subscript n denote depth, time and normalized respectively. The PE per unit mass is computed as $0.5\rho_o N^2\overline{\eta'^2}$, where $\overline{\eta'^2}$ is the variance of vertical displacements averaged over intraseasonal frequency band and ρ_o is averaged density across pycnocline depths. Kinetic energy (KE) is inferred from the spectra of v' and defined as $0.5\rho_o\overline{v'^2}$, where $\overline{v'^2}$ is variance attributed to v' averaged over intraseasonal periods. Vertical structures of PE and KE (Fig. 9) demonstrate that PE and KE have similar amplitudes, indicative of equipartition between PE and KE, which further supports our hypothesis that the Kelvin wave field contributes significantly to intraseasonal motion in the Makassar Strait thermocline.

3.3.4 Dispersion relation

The dispersion relation for a Kelvin wave in Makassar Strait, a North-South oriented channel, would be $\omega = \ell c$, where ℓ and c are wavenumber in the y direction and wave phase speed, signifying a constant phase speed or non-dispersive. We employ the v' datasets at Lombok and Makassar Straits to investigate whether the coherent oscillation transmitting from Lombok Strait to Makassar Strait reported by Pujiana et al. (2009) exhibits a dispersion relationship consistent with a Kelvin wave.

The v' time series at the upper 200 m of Lombok Strait and that at depths below 75 m of Makassar Strait are statistically coherent above the 95% significance level across the period band of 45-90 days, and the corresponding phase differences linearly decrease with period. For example, v' at 100 m in Lombok Strait and Makassar Strait are not only statistically coherent but also show a linear trend of decreasing phase difference with period (Fig. 10), indicative of a propagating feature with a quasi-constant phase speed of 1.3 ± 0.01 m/s from Lombok Strait to Makassar Strait (a distance of 1240 km, the 100-m isobath length connecting the moorings at Lombok and Makassar Straits, is used in the computation). Thus the relationship between ω and ℓ inferred from the coherence analysis exemplifies a non-dispersive wave.

In addition to the relation between ω and ℓ, the relation between ℓ and m (vertical wavenumber) is also useful to determine the wave classification. The equatorial wave dispersion relation, $(k^2N_o/m\beta)+(kN_o/\omega m)-(\omega^2 m/N_o\beta)+2n+1 = 0$, can be simplified as $k = -(2n+1)m\omega/N_o$, where k is zonal wavenumber, N_o is averaged stratification frequency over depths, m is vertical wavenumber, β is beta effect, and n is meridional mode number (n = -1, 1, 2, …). Because of the Makassar mooring's proximity to the equator, we propose that the equatorial wave dynamics are suitable to explain any waveforms captured in the study area. Nevertheless the wave properties are now assumed to vary zonally because the main axis of the Makassar Strait is nearly parallel to the y-direction, so the corresponding dispersion relation is $\ell = -(2n+1)m\omega/N_o$. The estimated ℓ and m at $\omega = 2\pi/60\text{-day}^{-1}$ obtained from coherence analyses of v' at Lombok and Makassar Straits also well approximate the Kelvin wave dispersion curve (Fig. 11).

3.3.5 Semi-geostrophic balance and increased decay scale

Observations and numerical experiments agree that the Kelvin wave energy originating in the equatorial Indian Ocean significantly influences the intraseasonal variability at Lombok Strait (Arief and Murray, 1996; Qiu et al., 1999, Schiller et al., 2010, Drushka et al., 2010). Drushka et al. (2010) proposed that the vertical structure of the observed Lombok Strait throughflow at intraseasonal timescales was best explained by a baroclinic Kelvin wave. We will be discussing two other Kelvin wave attributes measured at Lombok Strait: semi-geostrophic balance and reflected Kelvin wave.

A simple wave equation and its boundary condition applicable for simplified Lombok Strait, a channel bounded by vertical walls, are given as, $\frac{\partial^2\eta'}{\partial x^2}+\left\{\frac{-\omega^2-f^2}{c^2}-l^2\right\}\eta'=0$ and $\frac{\partial^2\eta'}{\partial x^2}+\left\{l(\frac{f}{\omega})\right\}\eta'=0, x=0, W$, where η' is sea level anomaly across the strait, *l* is wavenumber in the along-strait axis direction, and *W* is the strait width. The general solution, with $\omega = \pm lc$, is $\eta'(x,t)=\eta_o e^{-\frac{fx}{c}}\cos(ly-\omega t)$, where *c* denotes Kelvin wave phase speed. Given the corresponding momentum equation is $v'(f^2-\omega^2)-gf\frac{\partial\eta'}{\partial x}+g\frac{\partial^2\eta'}{\partial x\partial y}=0$ we can then obtain $v'=\frac{g}{f}\frac{\partial\eta'}{\partial x}$ which implies a semi-geostrophic balance.

The u', v' obtained from moorings, and η' from the pressure gauges and altimeter are employed to examine the Kelvin wave signatures in Lombok Strait. We focus on the May 2004 event during which the instruments were all operational. Moorings and pressure gauges in Lombok Strait demonstrated that $+v'$ and $+\eta'$ characterized the Lombok Strait intraseasonal variability during May 2004 (Fig 12). We also identify that the across-strait SLA slopes down towards the east ($\partial\eta'/\partial x < 0$), with higher sea level at

P_w than P_e, when $v' > 0$ during May 2004 (Fig. 12), indicative a balance between $\partial\eta'/\partial x$ and zonal coriolis force. Meanwhile the along-strait sea surface tilt ($\partial\eta'/\partial y$), inferred from satellite-derived SLA measured at two locations in Lombok Strait (P_n and P_s; Fig. 1), is not balanced by f in the y-direction as the sea surface slopes up towards the south ($\partial\eta'/\partial y < 0$) when $u' > 0$ (Fig. 12b and c; Fig. 13a), indicative of ageostrophy. Moreover the estimated geostrophic $+v'$ inferred from $\partial\eta'/\partial x$ does not differ significantly from $+v'$ measured from moorings (Fig. 13b), which confirms a partial geostrophic balance in the x-direction.

The two shallow pressure gauges at the zonal boundaries of Lombok Strait also indicated enhanced across-strait decay scale, another Kelvin wave attribute. The estimated η' variability at P_e, $\eta'_{Pe} = \eta'_{Pw}\, e^{-W/R}$; with $W = 0.3R$ is the distance between the two pressure gauges and R is Rossby radius of deformation, is less than the observed η'_{Pe} (Fig. 13c). The discrepancy between the measured and estimated η'_{Pe} implies increased across-strait decay scale. Durland and Qiu (2003) connected a low-frequency Kelvin wave passage in a strait with enhanced across-strait decay scale, mainly forced by the formation of a reflected Kelvin wave whose direction was 180° out of phase with the incident wave. When a Kelvin wave in Lombok Strait reaches an entrance into a larger basin, it does not contain the required energy to force a wave of equal amplitude in that basin which leads to the genesis of a reflected wave in order to preserve the continuity of pressure at the strait mouth. Since the maximum amplitude of the reflected wave is on the opposite side of the strait to the maximum amplitude of the incident wave, the reflection subtracts more from the minimum amplitude of the incident wave than it does from the maximum amplitude. This likely results in an enhanced across-strait pressure gradient such as observed in Lombok Strait (Fig. 13c).

4. Waveguide from Lombok Strait to Makassar Strait

We have demonstrated that observations at Makassar and Lombok Straits reveal intraseasonal motions with Kelvin wave signatures, which signify propagation from Lombok Strait to Makassar Strait. Discontinuous coastlines separate the moorings at both straits raising the question of the pathway guiding the wave from Lombok Strait to Makassar Strait. Given the averaged depth across section A (Fig. 14a) is 145 m, a barotropic Kelvin wave with a deformation radius of 1900 km would overcome the gap of ~475 km and force another barotropic Kelvin wave of reduced amplitude to propagate along the southern Kalimantan coasts into the Makassar Strait. In contrast the gap is too wide for the observed baroclinic Kelvin wave with a deformation radius of less than 100 km to "jump over".

A route which extends for 5195 km and runs along the northern Bali and Java, and eastern Sumatra coasts, the equator (across the South China Sea) and southern Kalimantan coasts (Fig. 14a) would serve as a viable waveguide for a baroclinic Kelvin wave originating in Lombok Strait because the gaps in Bali and Sunda Straits (Fig. 14a) are less than the deformation radius. Nevertheless the first two modes of a baroclinic Kelvin wave with a speed of 1.2-2.5 m/s would take at least 25 days to propagate along this waveguide, whereas the lags between the *v'* at Makassar Strait and that at Lombok Strait vary from 12-16 days (Fig. 14b), indicative a shorter pathway connecting both

Straits. The third mode of a baroclinic Kelvin wave with a speed of 0.8 m/s would take even longer.

A shorter pathway from Lombok Strait to Makassar Strait is along the isobaths, across the Sunda continental slope and at depths greater than 50 m (Fig. 14a), where a slope-trapped baroclinic Kelvin wave may propagate towards Makassar Strait with shallower water to the left. The propagation of a baroclinic Kelvin wave along an isobath has been studied through both laboratory experiments and observations (Codiga et al., 1999; Hallock et al., 2009). Fig. 14a depicts the 100-m isobath, which extends for ~1240 km and links the moorings in Lombok and Makassar Straits. A baroclinic Kelvin wave with a speed of 0.8-1.2 m/s, equivalent with a speed of the second and third modes theoretical baroclinic Kelvin waves inferred from stratification, would take 12-18 days to reach Makassar Strait, which is in good agreement with the observations (12-16 days, Fig. 14b). We thus speculate that the Kelvin wave propagates as the second and third baroclinic modes along the 100-m isobath directly linking Lombok to Makassar Strait.

5. Transport and mixing associated with Kelvin wave in Makassar Strait

5.1 Transport

We have provided supportive evidence for Kelvin wave propagation from the velocity vectors, temperature and stratification datasets. We now address a question of the relevance of Kelvin waves to ITF studies, more specifically, what are the transport anomalies associated with the intraseasonal baroclinic Kelvin waves in Makassar Strait? To deduce the estimated transport anomalies, we use the v' datasets at depths of 125-450 m from the Mak-West and Mak-East moorings. At each depth of z, we fit the v'

timeseries from both moorings using an exponential function of $v' = v'_{Mak-west}\ e^{-x/b}$, which results in the across-strait structure of *v'*, *v'* (*x*, *z, t*), where b is the horizontal scale coefficient, and *x* = 0:*L* (*x* = 0 and *x* = *L* correspond with the Mak-West and Mak-East mooring sites respectively). The transport is then computed as $\int_{z=-450}^{z=-150} \int_{x=0}^{x=L} v'(x,z,t)dxdz$. The transport variability observed during 2004-2006 across the pycnocline (Fig. 15) indicates that a downwelling intraseasonal Kelvin wave passage could drive northward mass transport of 0.75 ± 0.4 Sv (mean ± standard deviation) across depths of 125-450 m within the Makassar Strait pycnocline with a maximum northward transport of ~2 Sv recorded in late May 2005 (Fig. 15).

5.2 Mixing

Ffield and Gordon (1992), using an archive of CTD datasets and 1-D advection and diffusion equation, characterized tidal currents as the main forcing for the strong vertical mixing with vertical diffusivity in excess of 10^{-4} m^{-2}/s^{-1} in the Makassar Strait thermocline. At intraseasonal timescales, Figs. 4b-d, 5 and 6 demonstrate that a Kelvin wave episode in Makassar Strait is marked with the vertically sheared *v'*, which potentially yields unstable stratification through Kelvin-Helmholtz instability and contributes to the vertical mixing strength. In a steady, inviscid, non-diffusive, and stably stratified, small disturbances are stable provided the Richardson number, R_i = $N^2/(dv'/dz)^2$, is greater than ¼ everywhere in the fluid. The relationship between a Kelvin wave and Kelvin-Helmholtz instability arises from the Kelvin's wave perturbation to *v'* and *T'*. Thus if a Kelvin wave were important to govern the *v'* variation across the pycnocline depths in Makassar Strait, we would expect that the energetic wave episodes correspond with small R_i.

The R_i variability (Fig. 16) across the Makassar Strait pycnocline is computed using the observed *v'* and *N* at the Mak-West site, where *N* was computed by assuming ρ' is equivalent to *T'*. Fig. 16 demonstrates that the likelihood of unstable stratification within the lower pycnocline depths is greater during the period when observed Kelvin wave signatures are stronger in Makassar Strait (e.g. late May, August 2004, December 2004, June 2005, November 2005). Furthermore the corresponding eddy viscosity coefficient is parameterized using, $K_v = 5.6 \times 10^{-8} R_i^{-8.2}$, a formula appropriate in a region where density variations are dominated by those of temperature (Thorpe, 2004) such as in Makassar Strait, and the vertical diffusivity during strong Kelvin wave events varies from 1-5 $\times 10^{-5}$ m^2/s^{-1}.

6. Discussion and Summary

We have described the characteristics of the 2-3 month oscillations measured in Makassar Strait during 2004-2006, marking the weakened ITF transport across the pycnocline and the vertically sheared *v'* at the subpycnocline. A composite of the 17 +*v'* events found within the pycnocline depths exhibits an upward phase tilt, which implies a vertically propagating wave attribute with a non-local origin. The *v'* and *T'* data across the pycnocline show a quarter cycle of phase shift, which favors downward energy propagation, and also the kinetic-potential energy equipartition. Warmer pycnocline occuring during the +*v'* episodes is also evident from the relation between *v'* and *T'*. Furthermore a normal mode approximation is also applicable to explain the link between the vertical structure of v' and stratification. We suggest that these characteristics pertinent to the 2-3 month variability observed in the Makassar Strait are in agreement with the theoretical downwelling Kelvin wave signatures.

The η', u' and v' data in Lombok Strait also demonstrate two Kelvin wave attributes in the semi geostrophic balance between v' and $d\eta'/dx$ and in enhanced $d\eta'/dx$, which corroborates those reported by Drushka et al. (2010). The v' data in Lombok Strait and that in Makassar Strait are coherent and yield a Kelvin wave dispersion relationship between the wavenumber and wave frequency. The waves propagate from Lombok Strait to Makassar Strait with a phase speed of ~1.3 m/s, a 2nd mode baroclinic Kelvin wave speed. The 2nd baroclinic wave mode inferred from the measured Kelvin wave phase speed affirms the baroclinic vertical structure attributed to the $+v'$ events in Makassar Strait which exhibits two-zero crossing points over depths. Through the comparison of the $+v'$ episodes in Lombok Strait and Makassar Strait, we suggest that the Kelvin waves navigate along the 100-m isobath and extends for ~1240 km, to transmit its energy from Lombok Strait to Makassar Strait. Another shallower route, encompassing a distance of ~ 5195 km along the coasts of Java, Sumatra, and Kalimantan, is too long a pathway for a baroclinic Kelvin wave to propagate over within the 12-16 days, the lags that the $+v'$ events in Makassar Strait display relative to that in Lombok Strait. Thus the intraseasonal Kelvin waves in Makassar Strait are linked to that in Lombok Strait.

Drushka et al. (2010) demonstrated that the model v' data in Lombok Strait, simulated by a simple wind-forced model forced by zonal winds in the eastern equatorial Indian Ocean and along-shore winds along the Sumatra and Java coasts, showed a good agreement with observation. Because the intraseasonal motions in Makassar Strait and

Lombok Strait are significantly correlated, the intraseasonal Kelvin waves in Makassar Strait derive their energy from the same southeastern Indian Ocean winds.

Significant MJO phases preceded the Kelvin wave episodes in Makassar Strait occurring in March and May 2004; May, and September 2005 with the maximum $+v'$ at 150 m associated with the Kelvin wave trailing the peak of MJO by 19-25 days. Meanwhile the MJO leads $+v'$ at 150 m by 6-11 days, implying that the MJO's footprint in Makassar Strait lags that in Lombok Strait by 13-14 days, consistent with the number of days a baroclinic Kelvin wave requires to propagate from the Lombok Strait moorings to the Makassar Strait moorings. Unlike the study of Zhou and Murtugudde (2010), which suggested that the MJO affected the intraseasonal variability only at the ITF outflow passages such as Lombok Strait, we propose that the MJO-related oceanic Kelvin wave is also observed in Makassar Strait.

The downwelling Kelvin wave passages affect the ITF transport anomalies, in which a wave episode results in an averaged northward anomaly of ~0.75 Sv across the pycnocline depths of 100-450 m. The wave passages are also commensurate with the small Richardson number phases, during which dv'/dz is intensified amplifying the likelihood of Kelvin-Helmholtz instability resulting in a vertical mixing with K_z of 1-5×10^{-5} $m^2 s^{-1}$.

Acknowledgements

This work is supported by the National Science Foundation grant OCE-0219782 and OCE-0725935 (LDEO) and OCE-0725476 (SIO). The altimeter data were produced by SSALTO/DUACS and distributed by AVISO. The MJO index was obtained from

http://cawcr.gov.au/staff/mwheeler/maproom/RMM/RMM1RMM2.74toRealtime.txt).

This is Lamont-Doherty contribution number xxxx.

References

Arief, D., and S. P. Murray, 1996. Low-frequency fluctuations in the Indonesian throughflow through Lombok Strait, J. Geophys. Res., 101(C5), 12, 455-12, 464, doi:10.1029/96JC00051

Codiga, D. L., D. P. Renouard, and A. Fincham, 1999. Experiments on waves trapped over the continental slope and shelf in a continuously stratified rotating ocean, and their incidence on a canyon. J. Mar. Res., 57, 585-612.

Ducet, N., P. Y. Le Traon, and G. Reverdin, 2000. Global high-resolution mapping of ocean circulation from TOPEX/POSEIDON and ERS-1 and -2. J. Geophys. Res., 105 (C8), 19, 477-498.

Drushka, K., Sprintall, K., Gille, S., Brodjonegoro, I., 2010. Vertical Structure of Kelvin waves in the Indonesian Throughflow Exit Passages, J. Phys. Oceanogr., 40, 1965-1987.

Durland, T., and B. Qiu, 2003: Transmission of subinertial Kelvin waves through a strait. J. Phys. Oceanogr., 33, 1337–1350.

Ffield, A., and A. L. Gordon, 1992. Vertical Mixing in the Indonesian Thermocline, J. Phys. Oceanogr., 22, 184-195.

Gill, A. E., 1982. Atmosphere-Ocean Dynamics, Academic Press, NY, 662 pp.

Gordon, A.L. and Kamenkovich, V.M., 2010. Modelling and observing the Indonesian Throughflow. A special issue of Dynamics of Atmosphere and Ocean. Dyn. Atmos. Oceans, doi: 10.1016/j.dynatmoce.2010.04.003.

Gordon, A.L., Sprintall, J., Van Aken, H.M., Susanto D., Wijffels, S., Molcard, R., Ffield, A., Pranowo, W. and Wirasantosa, S., 2010. The Indonesian Throughflow during 2004-2006 as Observed by the INSTANT program. Dyn. Atmos. Oceans, doi: 10.1016/j.dynatmoce.2009.12.002.

Gordon, A.L. and Fine, R. A., 1996. Pathways of Water between the Pacific and Indian Oceans in the Indonesian Seas. Nature, 379, 146-149, doi: 10.1038/379146a0.

Gordon, A.L., Susanto, R.D., Ffield, A., Huber, B.A., Pranowo, W. and Wirasantosa, S., 2008. Makassar Strait Throughflow, 2004 to 2006. Geophys. Res. Lett., 35, L24605, doi: 10.1029/2008GL036372.

Gordon, A. L., Susanto, R.D., Vranes, K., 2003. Cool Indonesian throughflow as a consequence of restricted surface layer flow. Nature, 425, 824-828, doi: 10.1038/Nature02038

Gordon, A. L., 2005. Oceanography of the Indonesian Seas. Oceanography, 18(4):13, http://dx.doi.org/10.5670/oceanog.2005.18

Hallock, Z. R, Teague, W. J., Jarosz, E., 2009. Subinertial slope-trapped waves in the northeastern Gufl of Mexico. J. Phys. Oceanogr., 39, 1474-1485.

Pedlosky, J., 2003. Waves in the Ocean and Atmosphere, Springer-Verlaag, 276 pp.

Pujiana, K., Gordon, A.L, Sprintall, J. and Susanto, R.D., 2009. Intraseasonal variability in the Makassar Strait Thermocline. J. Mar. Res., 67, 757-777.

Qiu, B., Mao, M. and Kashino, Y., 1999. Intraseasonal Variability in the Indo-Pacific Throughflow and the Regions Surrounding the Indonesian Seas. J. Phys. Oceanogr., 29, 1599-1618, doi: 10.1175/1520-0485(1999)029<1599:IVITIP>2.0.CO;2.

Schiller, A., Wijffels, S.E., Sprintall, J., Molcard, R., Oke, P.R., 2010. Pathways of intraseasonal variability in the Indonesian throughflow region. Dynamics of Atmospheres and Oceans 50, 174-200, doi:10.1016/j.dynatmoce.2010.02.003.

Shinoda, T., Han, W., Metzger, E.J., and Hurlburt, H., 2012. Seasonal Variation of the Indonesian Throughflow in Makassar Strait. J. Phys. Oceanogr., in press.

Sprintall., A. L. Gordon, R. Murtugudde, and R. D. Susanto., 2000. A Semiannual Indian Ocean forced Kelvin wave observed in the Indonesian seas in May 1997. J. Geophys. Res., 105(C7), 17, 217-17, 230, doi: 10.1029/2000JC900065.

Sprintall, J., Wijffels, S., Gordon, A.L., Ffield, A., Molcard, R., Susanto, R.D., Soesilo, I., Sopaheluwakan, J., Surachman, Y. and Van Aken, H., 2004. INSTANT: A New International Array to Measure the Indonesian Throughflow. Eos Trans. AGU, 85(39), doi: 10.1029/2004EO390002.

Sprintall, J., S. Wijffels, R. Molcard, and I. Jaya, 2009. Direct estimates of the Indonesian Throughflow entering the Indian Ocean, *J. Geophys. Res.* , 114, C07001, doi: 10.1029/2008JC005257.

Thorpe, S. A., 2004. Recent Developments in the Study of Ocean Turbulence, Ann. Rev. Earth Planet. Sci., 32, pp. 91-109.

Wijffels, S., Meyers, G., 2004. An Intersection of Oceanic Waveguides: Variability in the Indonesian Throughflow Region. J. Phys. Oceanogr., 34, 1232-1253. doi: http://dx.doi.org/10.1175/1520-0485(2004)034<123:AIOOWV>2.0.CO;2.

Zhou, L. and R. Murtugudde, 2010. Influences of Madden-Julian Oscillations on the 782 eastern Indian Ocean and the maritime continent. Dyn. Atmos. Oceans, 50, 257-274.

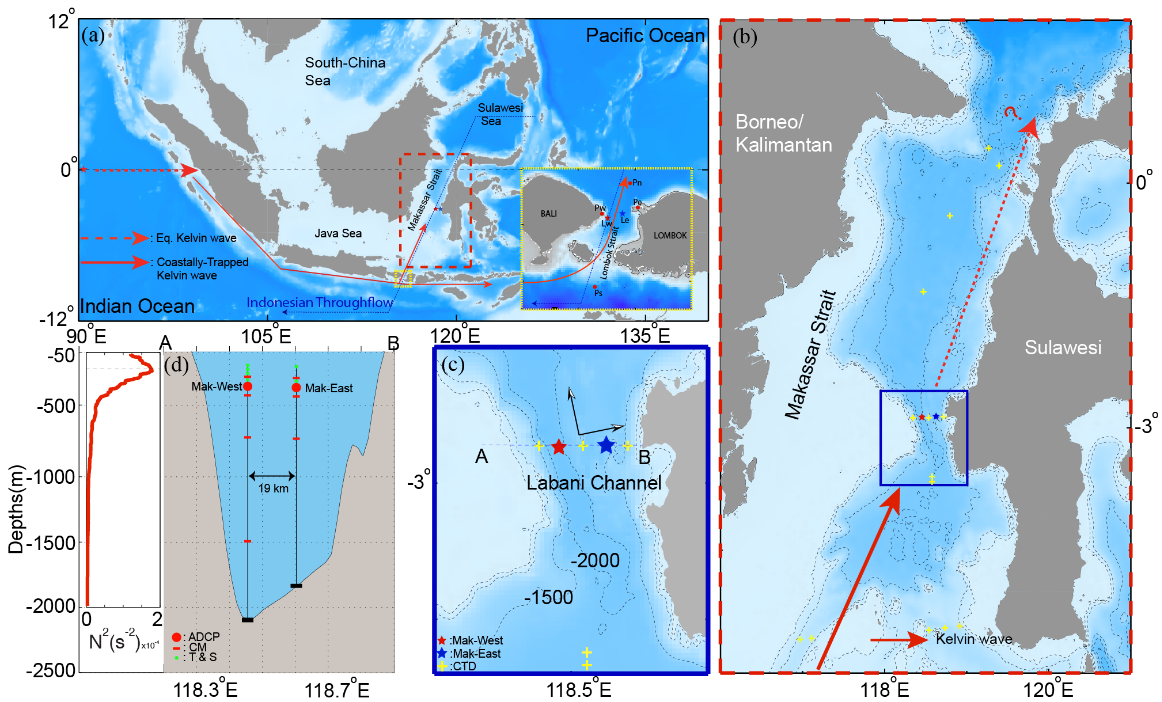

Fig.1. (a) The Makassar Strait location (dashed red box) in the maritime continent, and the schematic of the waveguide for the Kelvin wave (red arrow). Inset is an expanded view of Lombok Strait and the corresponding mooring (Lw and Le) and shallow pressure gauge (Pw, Pe, Pn, and Ps) sites. (b) A blow-up of the red dashed box in (a) showing Makassar Strait location and its bathymetric profiles. The blue box indicates the Labani Channel, where the moorings (stars) were deployed. Yellow crosses denote CTD stations. (c) Mooring sites in the Labani Channel. (d) A bathymetric cross-section A-B in the Labani Channel, mooring configuration, and an averaged stratification profile obtained from the CTD stations.

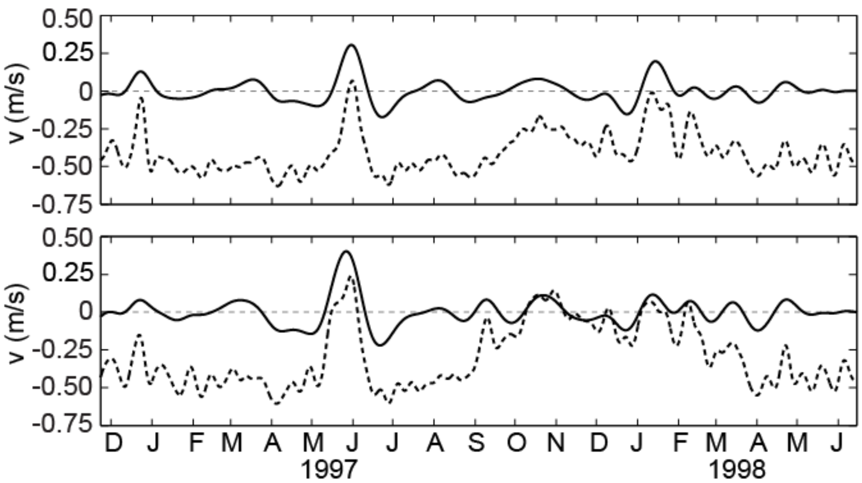

Fig. 2. Timeseries of subinertial (dashed) and intraseasonal (solid) along-strait flow at 250 m (upper panel) and 350 m (lower panel) at the Mak-West site. Positive velocity indicates northward flow. The data were observed during late November 1996 – mid June 1998.

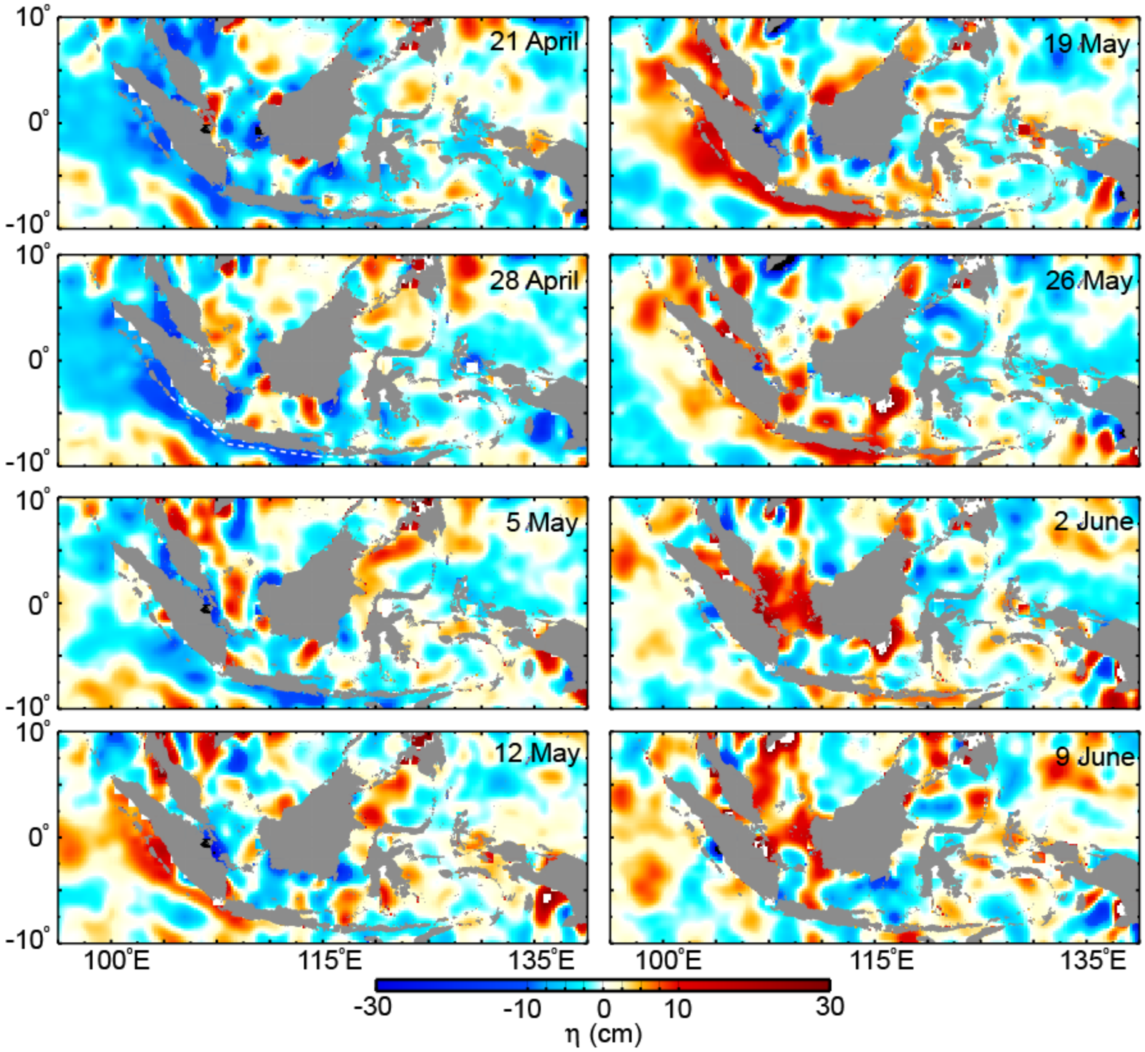

Fig. 3. Snapshots of satellite altimetry-derived SLA (η) over the maritime continent during 21 April-9 June 2004. The η data vary at intraseasonal timescales. The white dashed line on the 28 April snapshot denotes a section along which the CTKW phase speed is computed.

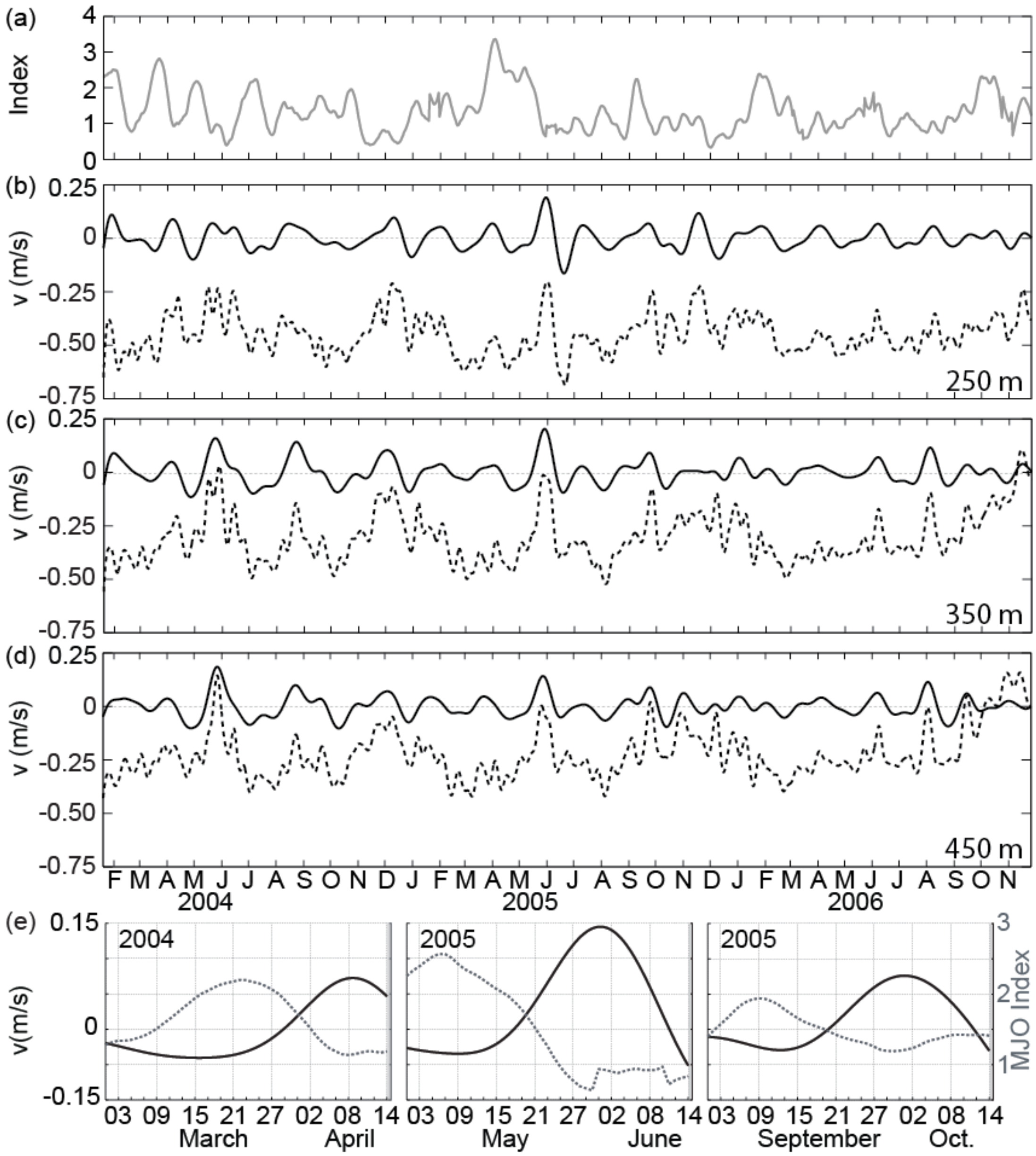

Fig. 4. (a) Timeseries of Madden-Julian Oscillation index. Timeseries of subinertial (dashed) and intraseasonal (solid) along-strait flow at b) 250, c) 350, and d) 450 m. The MJO and velocity data were observed from 20 January 2004 to 26 November 2006. (e) Plots of the intraseasonal along-strait flow timeseries (solid) at 150 m and MJO index (dashed) during strong MJO phases.

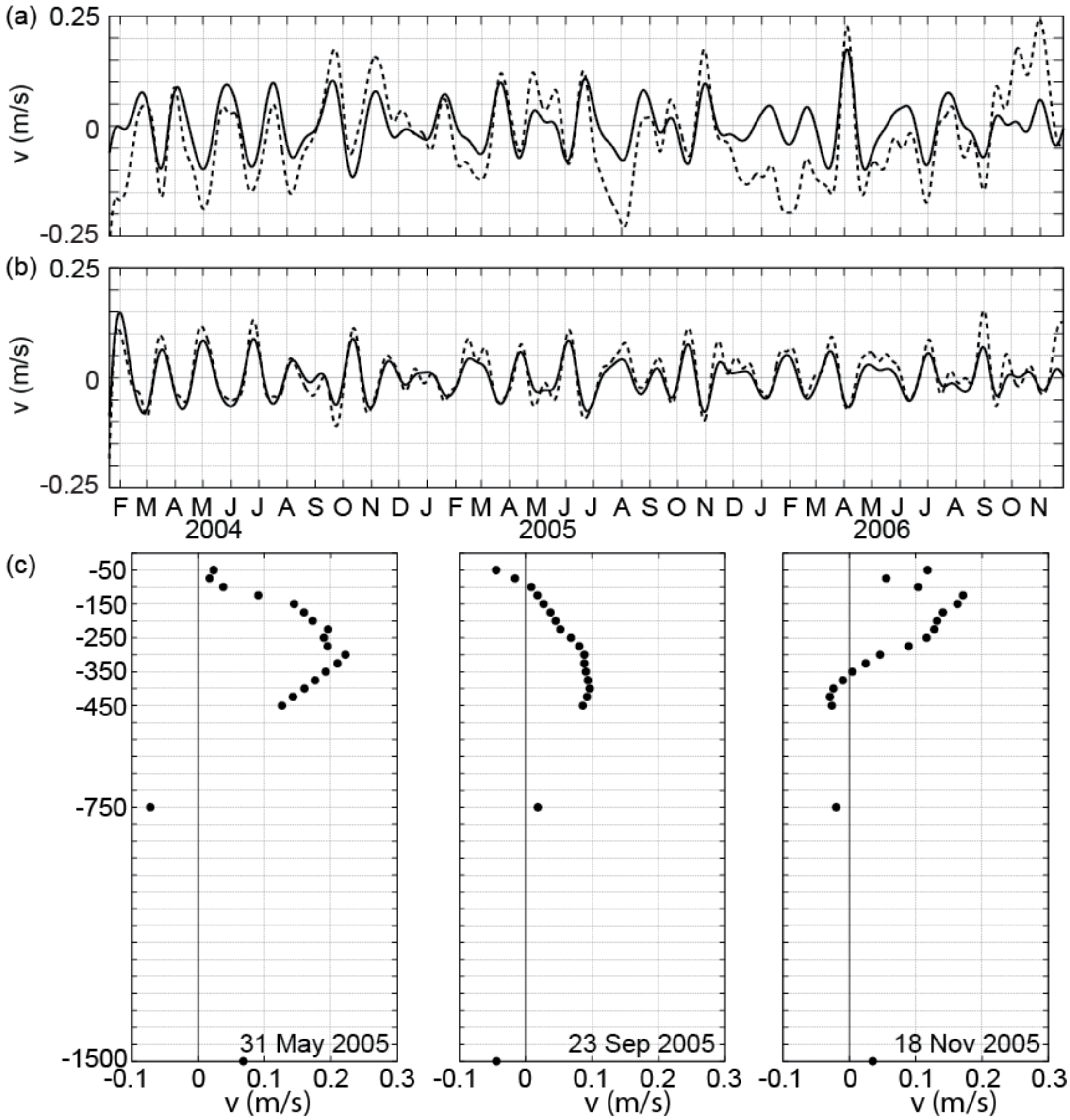

Fig. 5. The along-strait flow timeseries varying at subinertial (dashed) and intraseasonal timescales (solid) observed at 750 m (a) and 1500 m (b) within the Mak-West subpycnocline. (c) Vertical structure of the intraseasonal along-strait flow data across the pycnocline and at two subpycnocline depths at three events when the intraseasonal along-strait flow at the pycnocline attains maximum value.

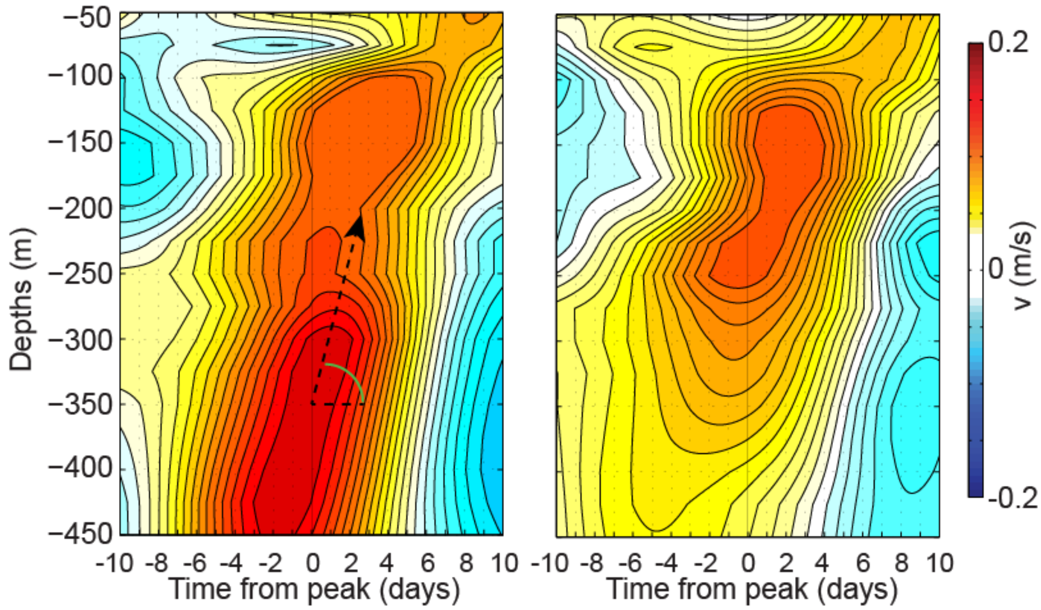

Fig. 6. The composite of the northward along-strait flow at intraseasonal timescales observed at the Mak-West (left panel) and Mak-East (right panel) pycnocline. Day 0 was defined as the time of the peak northward flow at 350 m. The dashed line with an arrow denotes the phase line, and the angle (green curve) that the line makes with the horizontal dashed line indicates upward phase shift of 50 m/day.

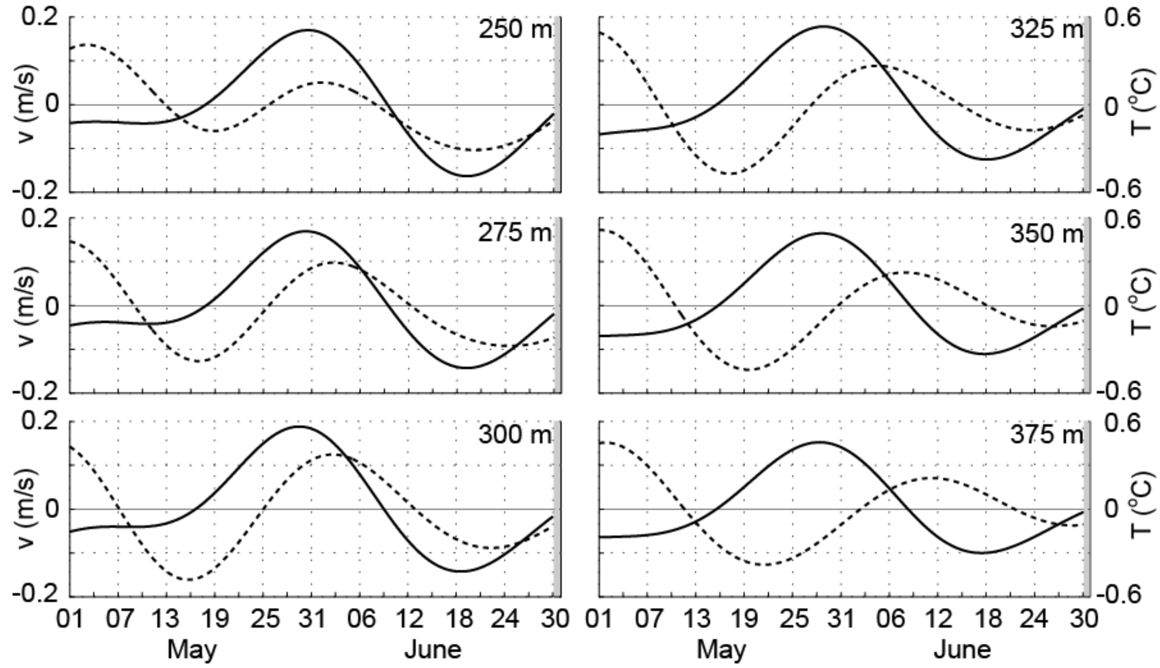

Fig. 7. The along strait flow (solid) and temperature (dashed) timeseries varying at intraseasonal timescales observed at several depths within the Mak-West pycnocline during May-June 2004. Positive velocity indicates northward flow.

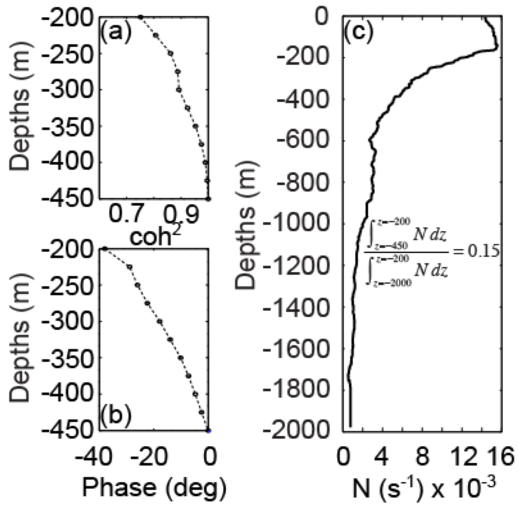

Fig. 8. (a and b) Coherence amplitudes and phases between intraseasonal along-strait flow at 200 m and that at deeper levels observed at the Mak-West lower pycnocline. The coherence amplitudes and phases are for along-strait flow at a period of 60-days. (c) An averaged profile of Brunt-Vaisalla frequency inferred from several Conductivity-Temperature-Depth (CTD) casts (yellow crosses in Fig.1) in Makassar Strait during 1996-1998.

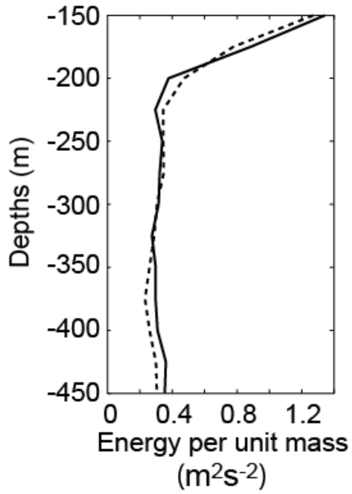

Fig. 9. Vertical structure of potential (solid) and kinetic (dashed) energy across the lower pycnocline. The potential and kinetic energy are inferred from temperature and along-strait flow varying at intraseasonal timescales observed at the Mak-West mooring.

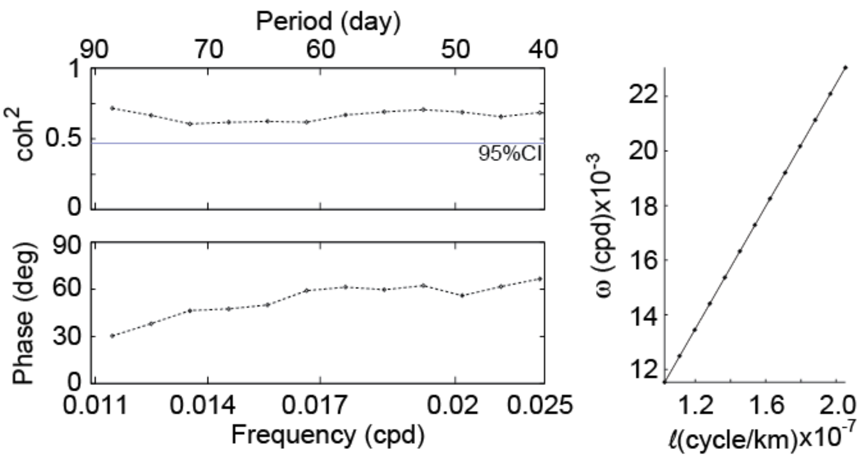

Fig. 10. (Left) Coherence amplitudes and phases between the intraseasonal along-strait flow timeseries at 100 m in Lombok Strait (Lombok-East/Le) and that at 100 m in Makassar Strait (Mak-West). (Right) Dispersion relation diagram inferred from the phase shift plot shown in the left panel.

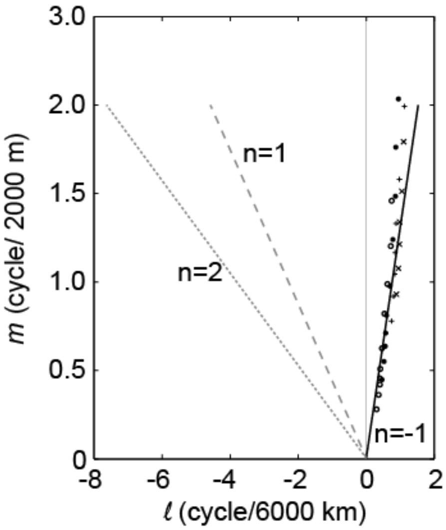

Fig. 11. Dispersion diagram of horizontal versus zonal wavenumber at $\omega = 2\pi$ 60 day^{-1}. The markers indicate the estimated values from the data, the solid black line demonstrates dispersion relation for a theoretical Kelvin wave, and the grey lines are the dispersion relation for the first two modes of theoretical Rossby waves.

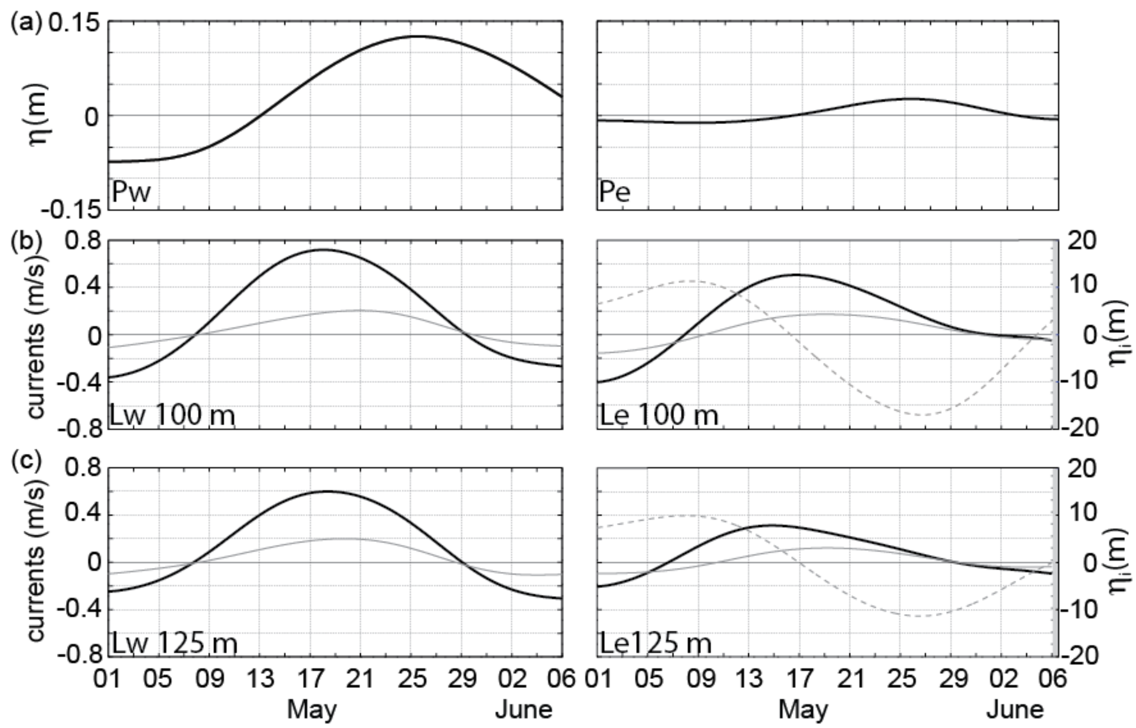

Fig. 12. (a) Time series of SLA at intraseasonal timescales during May-6 June 2004 from two shallow pressure gauges deployed in Lombok Strait, Pw and Pe. (b and c) Time series of along-strait flow (solid black), across-strait flow (solid grey) and vertical isopycnal displacements (dashed gray) varying at intraseasonal timescales observed at Lombok moorings.

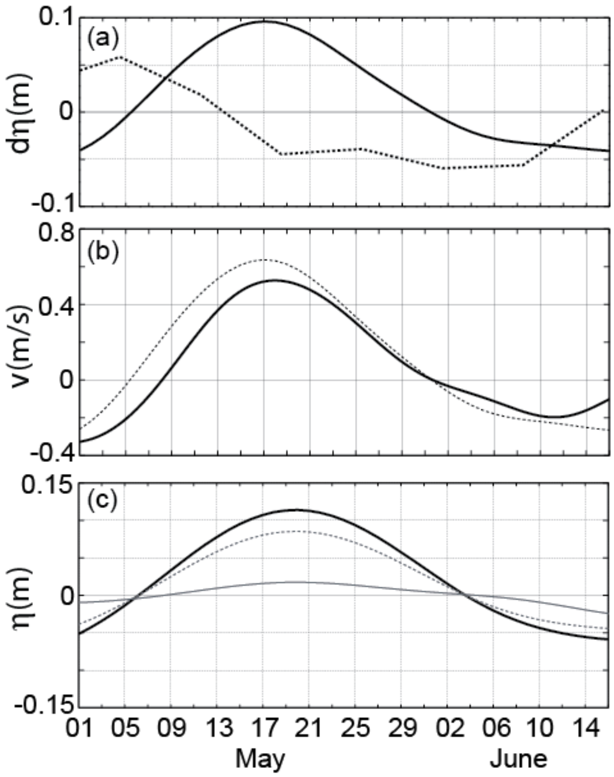

Fig. 13. (a) Across-strait gradient of SLA ($\eta_{Pw} - \eta_{Pe}$, solid) computed from the shallow pressure gauges and along-strait gradient of satellite altimetry derived SLA ($\eta_{Pn} - \eta_{Ps}$, dashed) in Lombok Strait. (b) Geostrophic flow inferred from the moorings (solid) and pressure gauges (dashed). (c) The observed η_{Pw} (black) and η_{Pe} (grey) and the estimated $\eta_{Pe} = \eta_{Pw}\, e^{-w/R}$ (dashed grey). (a,b, and c) demonstrate data from May-mid June 2004 which vary at intraseasonal timescales.

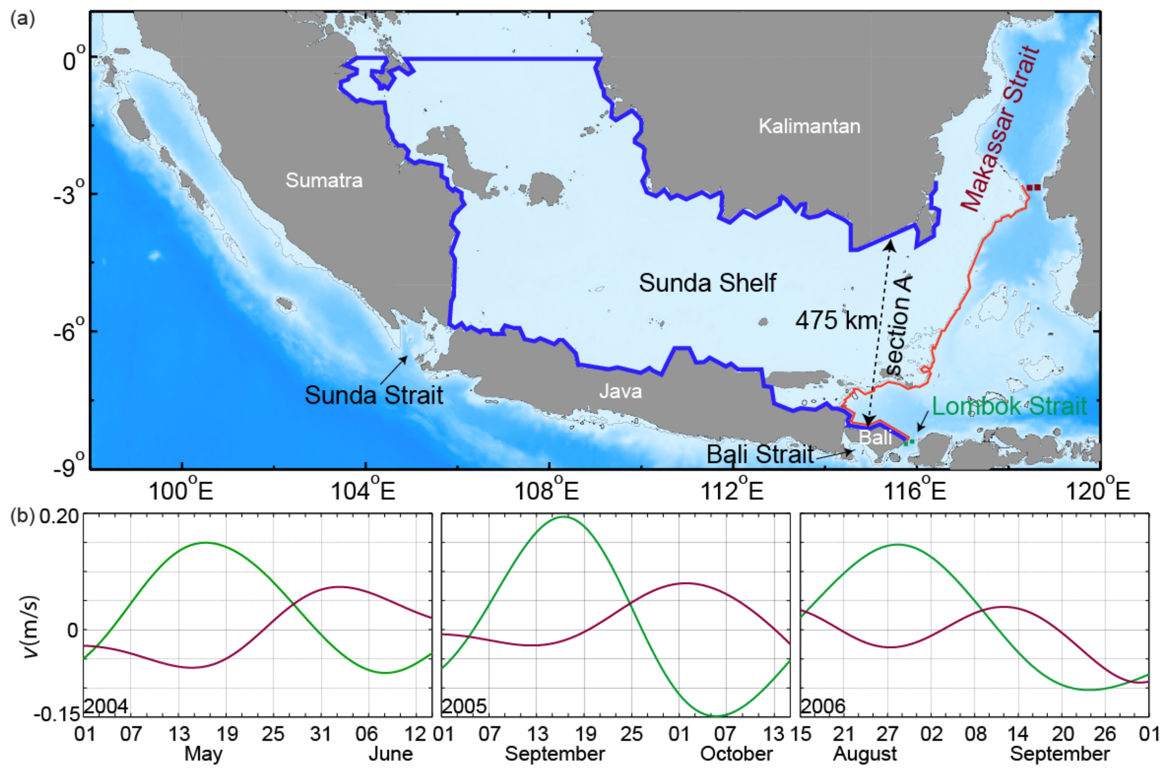

Fig. 14. (a) Potential pathways, route-1 (blue) and route-2 (red) for a Kelvin wave propagating from Lombok Strait to Makassar Strait. Route-1 extends for ~5195 km, while route-2 extends for 1271 km along the 100-m isobath. The colored boxes show the mooring sites, and the dashed contour depicts the 100-m isobath. (b) The intraseasonal along-strait flow data observed at 150 m of Lombok Strait (green) and Makassar Strait (purple).

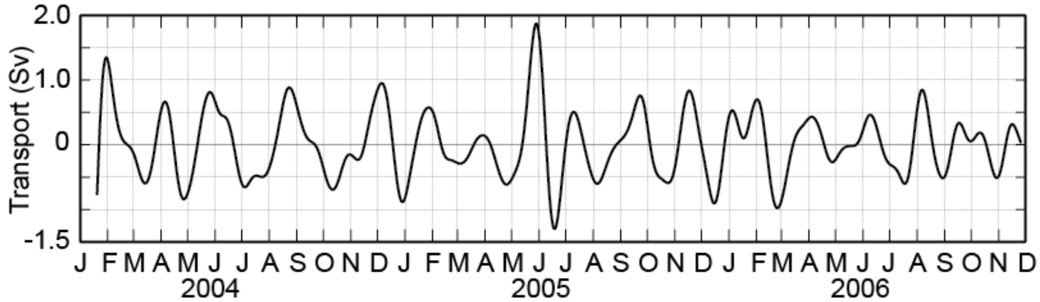

Fig. 15. The along-strait transport magnitudes varying at intraseasonal timescales estimated across the Makassar Strait pycnocline. The magnitudes express the transport anomalies attributable to intraseasonal Kelvin wave passages.

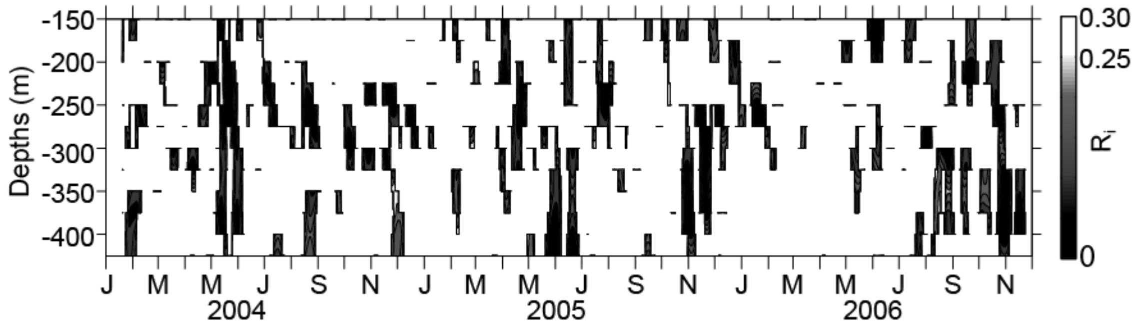

Fig. 16. Time series of R_i obtained from the ratio between the vertical shear of intraseasonal along-strait flow (d*v*'/d*z*) and *N* in the Makassar Strait pycnocline. The d*v*'/d*z* and *N* data are from the Mak-West mooring. $R_i > 0.25$ is given in white, while $R_i < 0.25$ is shown in grey/black.